NRL Report 7104

UNCLASSIFIED

Intrinsic Efficiency of Thermoluminescent Dosimetry Phosphors

WILLIAM H. LUCKE

Dosimetry Branch
Nuclear Physics Division

August 13, 1970

NAVAL RESEARCH LABORATORY
Washington, D.C.

This document has been approved for public release and sale; its distribution is unlimited.

UNCLASSIFIED

NRL Report 7104
Change 1
October 2, 1970

From: Naval Research Laboratory
To: Distribution List for NRL Report 7104, "Intrinsic Efficiency of Thermoluminescent Dosimetry Phosphors," by William H. Lucke, August 13, 1970

1. Page 2, 1st paragraph, 7th line, under the section "PROCEDURE AND APPARATUS," change 250 R/hr for $Li_2B_4O_7$ to read 520 R/hr for $Li_2B_4O_7$.

2. Page 30, 5th paragraph, 5th line, change (60 m) to (60 mg).

3. Page 34, Eq. (A1), (A2), and 1st paragraph, change $\int_0 FdA$ to $\delta F)_{dA}$

In last equation page 34, change $\int_0 A$ to δA

DEPARTMENT OF THE NAVY

NAVAL RESEARCH LABORATORY
Washington, D.C. 20390

OFFICIAL BUSINESS

POSTAGE AND FEES PAID
DEPARTMENT OF THE NAVY

CONTENTS

Abstract ii
Problem Status ii
Authorization ii

INTRODUCTION 1

EXPERIMENTAL APPROACH 1

PROCEDURE AND APPARATUS 2

Energy Absorbed 2
Apparatus for Determining Energy Emitted as Light 3
Heating Circuit 5
Optics 5

RESULTS 27

Calculation of Efficiencies 27
Relative Efficiency 27
Discussion 28

ACKNOWLEDGMENTS 31

REFERENCES 32

APPENDIX A — Justification for Expressing the Source Intensity in Watts/Steradian Instead of Watts/Cm^2 34

APPENDIX B — Proof that the Ratio of Detected Flux to Intensity is the Same for Both Lambertian and Isotropic Sources 37

UNCLASSIFIED

ABSTRACT

The intrinsic efficiency is defined as the ratio of light energy emitted during heating to energy absorbed during gamma irradiation. This factor was measured for four commonly used thermoluminescent phosphors to give the following results: LiF(TLD-100), 0.039%; $Li_2B_4O_7$:Mn, 0.073% (both corrected for supralinearity); CaF_2 Mn, 0.44%; and $CaSO_4$:Mn, 1.2%. The method of measurement involved calibrating a detector, which consisted of a narrow bandpass filter in conjunction with a photomultiplier, by means of the light of a standard lamp diffusely reflected from a MgO button having the same size, shape, and position as the phosphor-bearing planchet. A correction was made to account for the fact that the phosphor samples were not Lambertian sources.

PROBLEM STATUS

This is a final report on the problem. Unless the Laboratory is otherwise notified, this problem will be considered closed 30 days after the issuance of this report.

AUTHORIZATION

NRL Problem H01-24
Problems RR 002-06-41-5009 and
AEC (AT-49-7)-1864

Manuscript submitted March 23, 1970.

UNCLASSIFIED

INTRINSIC EFFICIENCY OF THERMOLUMINESCENT DOSIMETRY PHOSPHORS

INTRODUCTION

The application of the phenomenon of thermoluminescence to the measurement of ionizing-radiation exposure is relatively recent. In the early stages of development the efficiency of this process was immaterial. All that was needed was the knowledge that a given phosphor had, or had not, adequate sensitivity to measure the dose desired, and this was easily determined on a purely practical basis. Coupled with the lack of immediate need was the difficulty of obtaining meaningful measurements. The determination of light intensity as a function of wavelength is a difficult problem. When the low light level and transience of thermoluminescence are further considered, the problem becomes a formidable one indeed.

It appears now, however, that a stage has been reached at which efficiency measurements can yield fruitful results. Not only can comparisons between phosphors be made with a view of selecting the best for a particular application but also such knowledge can be helpful in gaining a theoretical understanding of the processes involved in thermoluminescence, thereby aiding in the search for new and better phosphors.

Only four previous attempts have been made to measure the intrinsic efficiency (1-4) of any of the phosphors treated here: LiF(TLD-100), manufactured by the Harshaw Chemical Company, Cleveland, Ohio; $Li_2B_4O_7$:Mn, manufactured by E.G. & G., Goleta, California; CaF_2 :Mn (NRL), and $CaSO_4$:Mn (NRL).

EXPERIMENTAL APPROACH

In this report, the intrinsic efficiency of a phosphor is defined as the ratio of the energy emitted as light during thermoluminescence (TL) to the energy absorbed (i.e., dose) during exposure to ionizing radiation. The latter quantity may be calculated easily, provided that (a) an accurately calibrated γ-radiation field is available and (b) the conditions for charged-particle equilibrium (CPE) are met. The procedures for achieving CPE, based on the well-known Bragg-Gray theorem, are, along with the coefficients necessary for its application, available in the literature (5).

The determination of the total light emitted during thermoluminescence is on the other hand quite complicated and subject to considerable error. Fundamentally, a light detector is calibrated by means of a light source of known intensity; then, from the response of the detector to the light of unknown intensity, the value of the latter can be inferred. The low light levels involved in TL require the use of a photomultiplier (PM) tube as a detector. The advantage of this device is, of course, high gain with low noise; however, its major disadvantages are (a) the area and effective location of the photocathode (which may vary in sensitivity from point to point) are never well known and (b) the gain depends on the wavelength of the incident light, is very sensitive to slight

Note: This research was originally presented at the 2nd Int. Conference on Luminescence Dosimetry, Gatlinburg, Tennessee, Sept. 23-26, 1968.

changes in the applied voltage, and is influenced by ambient-temperature and light-fatigue effects.

The difficulty arising from uncertainties in the photocathode was circumvented by an adaptation* of the well-known optical procedure of using a MgO plaque as a diffuse reflector. In our case the circular plaque of precisely known area, illuminated by a calibrated lamp, served as the standard for calibration of the PM tube. The plaque was then replaced by a circular planchet of exactly the same area, covered with phosphor. Thus, the solid angle subtended at the planchet by the photocathode was the same for both the plaque and phosphor and did not need to be known. This does not, however, solve the problem of calculating the total light emitted by the phosphor from a knowledge of the PM- tube response. It turns out that, while the plaque is a perfectly diffuse (or Lambertian) source, the phosphor is not — particularly for a very small phosphor mass — and this fact has to be taken into account.

To overcome the dependency of PM-tube gain on wavelength, narrow bandpass filters were used so that the light was nearly monochromatic and the detector was, in effect, no longer a PM tube alone, but a PM tube plus filter. This latter fact means, of course, that only the portion of the phosphor spectrum passed by the filter was measured. It was necessary to calculate the energy in the total emission spectrum from a knowledge of the energy passed by the filter. Fortunately Gorbics' (6) relative spectra of the phosphors investigated are available, and from them, and a knowledge of the filter transmission characteristics, this total energy was calculated.

Instabilities in the PM-tube gain, caused by small disturbances in supply voltage, temperature, etc., were overcome by using an internal luminescent light source so arranged that the gain of the system could be checked quickly and accurately before and after each measurement.

PROCEDURE AND APPARATUS

Energy Absorbed

As has been stated, calculation of the energy absorbed during irradiation requires both an accurately known radiation field and a knowledge of the conditions for CPE. Our γ radiation was obtained from a 200 Ci ^{60}Co source. The radiation field at known distances was measured by means of a carbon chamber whose sensitivity was determined by exposure to a standard NBS ^{60}Co field (7). The absolute accuracy of these measurements of our field is at least 5%. Exposure was at a rate of about 250 R/hr for CaF_2:Mn and LiF(TLD-100) and about 250 R/hr for $Li_2B_4O_7$:Mn and $CaSO_4$:Mn. The possible errors in the exposure time are assumed to be negligible.

To insure that CPE existed the phosphors were exposed in cups with heavy walls and covers of the appropriate material and thickness; 0.60 cm of graphite for the lithium-based phosphors and 0.64 cm of aluminum for the calcium-based ones. Corrections were applied for attenuation in the Lucite support, the cup wall, and the half-thickness of the phosphor. Under these conditions the absorbed dose deposited per roentgen of exposure of a phosphor ϕ is given by

*Suggested by S.G. Gorbics and R.J. Ginther (NRL).

UNCLASSIFIED

$$D_\phi = 0.869 \left[\frac{(\mu_{en}/\rho)_\phi}{(\mu_{en}/\rho)_{air}} \right]_{E_\gamma} \quad (1)$$

where

D_ϕ = absorbed dose (rad) deposited in the phosphor

0.869 = rad per roentgen (R) in air under CPE conditions

$(\mu_{en}/\rho)_{\phi,air}$ = the mass energy-absorption coefficients of the phosphor and air, respectively

These quantities are evaluated at the average energy of the incident ^{60}Co γ rays, which is 1.25 MeV. The effect of lower-energy scattered radiation was negligible in the source facility used in this experiment (8). Table 1 gives the values of μ_{en}/ρ for air and the phosphors investigated, as calculated from Hubbell's data (9), along with the conversion constant calculated from Eq. 1, the exposure, and the energy absorbed in ergs/g.

Table 1
Calculation of γ-Ray Energy Absorbed in Phosphors

Substance	μ_{en}/ρ*	rad/R	Exposure (R)	Energy Absorbed (ergs/g)
Air	0.0266	0.869	—	—
LiF(TLD-100)	0.0247	0.807	5.14×10^3	4.15×10^5
$Li_2B_4O_7$:Mn	0.0260	0.849	2.50×10^4	2.12×10^6
CaF_2:Mn	0.0259	0.846	4.00×10^3	3.38×10^5
$CaSO_4$:Mn	0.0267	0.869	3.60×10^2	3.13×10^4

*Mass energy-absorption coefficients were calculated from Hubbell's data (9).

Apparatus for Determining Energy Emitted as Light

PM Tube and Luminescent Standard — The PM tube used was an EMI side-window type 9662B, selected for low dark current (about 0.5 nA) and operated by using a well-stabilized supply with the cathode at 940 V negative. The bleeder current was 100 μA, and the anode current was allowed to rise to about 3% of this value on only one occasion; i.e., when calibration readings were being taken for the broad-bandpass 500-nm filter, anode currents of 5 to 6 μA were encountered. The calibration was completed using these values, and then the PM-tube voltage was lowered enough to decrease the gain by a factor of 10, and a new calibration run was made. The two calibrations agreed, indicating that PM-tube saturation effects were negligible at least up to a few microamperes in anode current.

The arrangement of the optical system is shown schematically in Fig. 1. Minor variations in light sensitivity of the PM tube were detected by means of a radioluminescent light source,* consisting of CaF_2:Mn powder mixed with ^{14}C inside a glass ampul embedded in a Lucite rod. Beta rays from the ^{14}C cause the CaF_2:Mn to emit blue-green light of practically constant intensity. The PM-tube housing was modified so that this "light checker" could be inserted opposite the end of the tube, the light being reflected by a coating of white TiO_2 paint on the inside of the tube housing. The resulting response was about 40 times the dark current. The inner end of the Lucite rod was painted black to serve as a shutter when the rod was partially withdrawn.

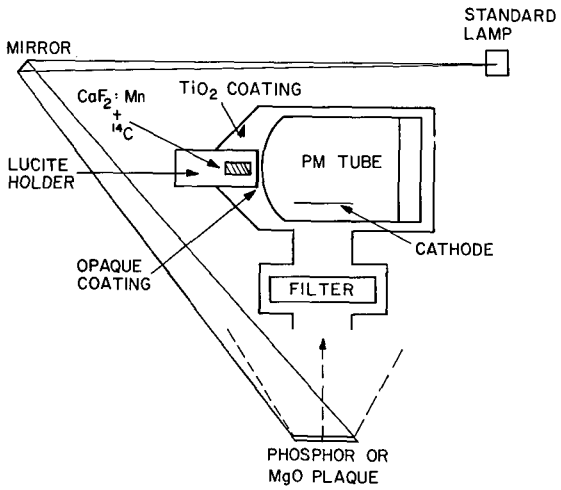

Fig. 1 - Diagram of the experimental arrangement. The shutter located below the filter is not shown. The figure is not drawn to scale.

A typical light-measuring sequence consisted of these five steps:

(1) The light-checker response current was integrated for 4 minutes,

(2) The dark current was integrated for 4 minutes,

(3) The response current to the reflected light from the MgO plaque was integrated for 4 minutes or the current was integrated during the emission of thermoluminescence by the phosphor sample,

(4) Repeat of (2),

(5) Repeat of (1).

The dark current readings were averaged and subtracted from each of the other readings, taking into account differences (from 4 minutes) in light exposure duration which occurred in the thermoluminescence measurements. The average net current from the PM tube during exposure to the light checker was next computed and used to divide the result of step (3) above to compensate for minor fluctuations which might occur in the PM-tube gain.

As indicated in Fig. 1, the interference-type filters were mounted between the shutter and the tube. The system was so designed that only a circular area about 1.9 cm in

*Edgerton, Germeshausen & Grier, Inc., Santa Barbara, California (commercial source).

UNCLASSIFIED

diameter at the center of the 2-in.-square filters was used. By this means the broadening of the passband arising from large angles of incidence was avoided.

Current Integrator — The output current of the PM tube was fed into an integrator* (Fig. 2), the first stage of which consisted of a chopper-stabilized negative-feedback amplifier which furnished the input to both the recorder and the integrator section. The latter was arranged to give one count per second on a six-digit register for full deflection on any of 12 current scales, ranging from 3×10^{-10} to 1×10^{-4} A. A meter afforded two-digit interpolation of charge between unit counts. Specifications were 0.3% precision of charge measurement, maximum drift of 0.02% per hour, and maximum input voltage 1 mV.

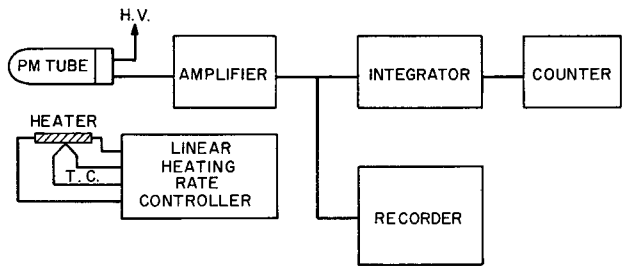

Fig. 2 - Diagram of electric and electronic circuits

A time-based recorder was used to monitor the progress of the glow curves and to determine when the integration was to be terminated. This was done manually when it was evident that the glow peak being measured was completely "glowed out." Figures 3a through 3d show typical glow curves obtained in these measurements, with integrated portions indicated by shading.

Heating Circuit

The linear heating-rate control circuit has been described by Gorbics, et al. (10). All glow curves in the present work were run at the heating rate of 80°C/min. The support for the graphite heating strip used by Gorbics was, however, modified so that the planchet was in full view of the PM tube.

Optics

The Source Characteristics — Before describing the experimental procedures further, it is necessary to discuss in some detail their theoretical basis. As we have said, the present method is based on the comparison of the light from a thin layer of phosphor with the light diffusely reflected at the surface of a uniformly illuminated MgO plaque. Considering both as sources, the energy emitted by each is distributed in a characteristic way among the various wavelengths present in its spectrum. There is also a distribution of energy in space (i.e., as measured in various directions with respect to the source), independent of the spectral one. Because of this independence the spatial distribution will be discussed without reference to wavelength, it being understood that the quantities introduced are defined for an infinitesimal range of wavelengths. The spectral distribution will be handled in a succeeding section.

*Model A310C, Halliburton Co., Silver Spring, Maryland.

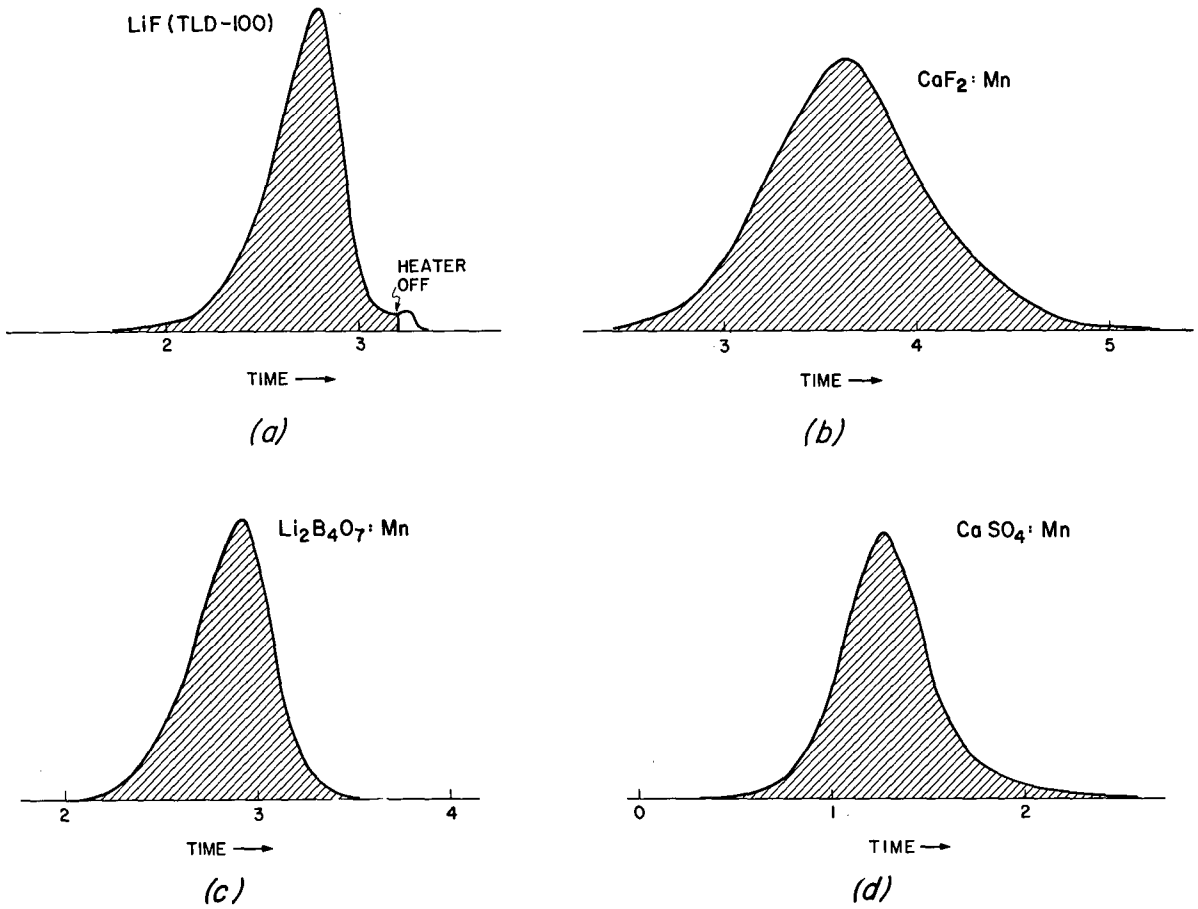

Fig. 3 - Display of typical recorder traces of the phosphors studied. Shading indicates area integrated.

It is generally accepted that at sufficiently large distances (in Appendix A it is shown that this condition is satisfied in the present experiment), a uniformly illuminated, circular MgO plaque gives a spatial distribution of radiant energy which is accurately described by Lambert's law; i.e.,

$$I_L = I_{L_0} \cos \theta \ , \tag{2}$$

where

θ = the angle between the normal to the plaque surface at its center and the line joining the plaque center to the center of the light detector

I_{L_0} = the intensity in ergs/sec-srad viewed along the normal to the plaque

I_L = the intensity seen by the detector at the angle θ

The total energy flux F_L (in ergs/sec) radiated into the upper hemisphere centered at the plaque is given by

UNCLASSIFIED

$$F_L = \int_0^{\pi/2} I_L \, d\omega = 2\pi I_{L_0} \int_0^{\pi/2} \cos\theta \sin\theta \, d\theta$$

$$= \pi I_{L_0} \sin^2\left(\frac{\pi}{2}\right) = \pi I_{L_0} , \tag{3}$$

where $d\omega$ = an element of solid angle in steradians, taken as $2\pi \sin\theta \, d\theta$ because of the circular symmetry.

If on the other hand we have a circular source of the same dimensions which does not follow Lambert's Law, Eq. 2 must be generalized to

$$I = I_\phi f(\theta) ,$$

where

θ is as defined for Eq. 2

$f(\theta)$ = some function of θ defined so that $f(0) = 1$

I_ϕ and I are defined as for I_{L_0} and I_L, respectively, in Eq. 2

In this case the total flux emitted into the upper hemisphere is given by

$$F_\phi = 2\pi I_\phi \int_0^{\pi/2} f(\theta) \sin\theta \, d\theta . \tag{4}$$

Evidently $f(\theta)$ must be known before the total energy can be calculated. For the special case of an isotropic source, $f(\theta) = 1$ and $F_\phi = 2\pi I_\phi$. Thus for a Lambertian versus isotropic source of the same output $F_L = F_\phi$; the intensities at $\theta = 0$ degree are related by $I_\phi = I_{L_0}/2$.

Since in the present problem the task is to calculate the total light flux from a knowledge of the flux incident on the detector, the fraction representing the ratio of the detected flux to the total flux radiated must be found. Rigorously the flux for the plaque should be written as

$$F_{L_c} = 2\pi I_{L_0} \int_0^{\theta_c} \cos\theta \sin\theta \, d\theta$$

where

F_{L_c} = the flux (ergs/sec) falling on the photocathode

θ_c = the angle subtended at the center of the plaque by the radius of the photocathode (assumed to be circular)

The flux for the phosphor-covered planchet is

$$F_c = 2\pi I_0 \int_0^{\theta_c} f(\theta) \sin\theta \, d\theta$$

Unfortunately the photocathode is not circular (being a rectangle nominally 0.95 cm×2.5 cm), so the integrations cannot be carried out as written. Moreover, the form of $f(\theta)$ is not known for the phosphor-covered planchet. However, as will be discussed later, enough may be deduced concerning $f(\theta)$ for small angles that, as shown in Appendix B, the detected fluxes are given with quite acceptable accuracy by

$$F_{L_c} = \pi I_{L_0} c \tag{5}$$

and

$$F_c = \pi I_0 c \ , \tag{6}$$

where c is a geometric factor ($\approx$0.00336).

The factor I_0 is, however, a function of the time, so Eq. 6 must be integrated over t_g, the time required to run a glow curve; hence,

$$\int_0^{t_g} F_c \, dt = \pi c \int_0^{t_g} I_0 \, dt$$

or

$$E_c = \pi c \Phi' \ , \tag{7}$$

where E_c is the total energy (ergs) falling on the photocathode in the course of a glow curve and Φ' is the energy intensity (ergs/srad) along the normal to the planchet.

The corresponding integration of Eq. 4 gives

$$E_\phi = 2\pi\Phi' \int_0^{\pi/2} f(\theta) \sin\theta \, d\theta$$

$$= \frac{\pi\Phi'}{G} \ , \tag{8}$$

where E_ϕ is the total energy (ergs) emitted by the phosphor into the upper hemisphere containing the PM tube and

$$G = \left[2 \int_0^{\pi/2} f(\theta) \sin\theta \, d\theta \right]^{-1} \tag{9}$$

and has the dimension of reciprocal steradians. As will be shown later, G is a function of the mass of the phosphor sample.

Combining Eqs. 7 and 8 yields

$$E_c = c E_\phi G \ . \tag{10}$$

The time integration of Eq. 5 is handled differently. What is desired is a unit of energy (called here the standard lamp unit and abbreviated SLU) in terms of which the phosphor output may be expressed directly, thereby avoiding explicit calibration of the PM tube. (This approach will be justified in the next section.) Multiplying both sides of Eq. 5 by 1 sec gives

UNCLASSIFIED

$$E_{L_c} = \pi c I_{L_0} \times 1 \text{ sec}$$
$$= \pi c S' \tag{11}$$

Thus, S' is the energy intensity (ergs/srad) along the normal to the plaque for a time of 1 sec.

Correspondingly Eq. 3 becomes

$$E_L = \pi S' \equiv 1 \text{ SLU} \tag{12}$$

Combining Eqs. 11 and 12 gives

$$E_{L_c} = c E_L \ . \tag{13}$$

The ratio of Eq. 10 to 13 is then

$$\frac{E_c}{E_{L_c}} = \frac{E_\phi G}{E_L} \ . \tag{14}$$

Clearly E_ϕ, the energy emitted by the phosphor into the upper hemisphere, must depend linearly on the mass m, assuming the phosphor layer to be thin enough not to produce significant internal absorption of light. Thus,

$$E_\phi = \Omega m \ ,$$

where Ω has the units ergs/g. This is converted to SLU by dividing by E_L; i.e.,

$$\frac{E_\phi}{E_L} = \frac{\Omega}{E_L} m$$
$$= \alpha' m \ , \tag{15}$$

where α' has the units SLU/g.

The final form of Eq. 14 is thus

$$\frac{E_c}{E_{L_c}} = \alpha' m G \ . \tag{16}$$

The Filters — The rationale behind the development of Eq. 16 is that the ratio E_c/E_{L_c} is given by the ratio of the integrated PM-tube outputs excited by the phosphor glow curve and a 1-sec standard lamp exposure, respectively. For the sake of clarity the derivation was carried through as though the light were monochromatic. To achieve this in practice, narrowband interference filters were used. The only change required in the derivation is that the quantities Φ' and S' be replaced by Φ and S, where

$$\Phi' = \int_{\lambda_{min}}^{\lambda_{max}} \Phi(\lambda)\, q(\lambda)\, d\lambda$$

and

$$S' = \int_{\lambda_{min}}^{\lambda_{max}} S(\lambda)\, q(\lambda)\, d\lambda ,$$

in which $\Phi(\lambda)$ is the energy intensity per wavelength of the light from the phosphor (erg/srad-nm), $S(\lambda)$ is the equivalent quantity for the illuminated plaque, per second of light exposure, and $q(\lambda)$ is the filter characteristic (dimensionless) having nonzero values in the interval λ_{min} to λ_{max} (in nanometers). Thus, the ratio of E_c/E_{L_c} is

$$\frac{E_c}{E_{Lc}} = \frac{\int_\lambda \Phi q\, d\lambda}{\int_\lambda Sq\, d\lambda} , \tag{17}$$

where, for convenience, the wavelength dependence of Φ, S, and q are understood along with the integration from λ_{min} to λ_{max}.

Evidently the integrated output of the PM tube Q_ϕ, when exposed to the phosphor, is

$$Q_\phi = \pi c \Gamma(\lambda_0) \int_\lambda \Phi q\, d\lambda , \tag{18}$$

and when exposed to the plaque

$$Q_L = \pi c \Gamma(\lambda_0) \int_\lambda Sq\, d\lambda , \tag{19}$$

where Q_L is the integrated output of the PM tube (in coulombs) when exposed for 1 sec to the plaque and $\Gamma(\lambda_0)$ is the gain in the PM tube and integrator (coul/erg), at the center wavelength λ_0, of the filter passband.

The ratio of Eq. 18 to Eq. 19 gives the experimentally measured quantity L:

$$L = \frac{Q_\phi}{Q_L} = \frac{\int_\lambda \Phi q\, d\lambda}{\int_\lambda Sq\, d\lambda} ,$$

and by comparison with Eqs. 17 and 16

$$L = \alpha' m G . \tag{20}$$

In the derivation of Eq. 20 it was assumed that the passband of the filter was narrow enough that the different spectral dependences of $\Phi(\lambda)$ and $S(\lambda)$ could be ignored and Eqs. 18 and 19 could be used instead of the rigorous inclusion of $\Gamma(\lambda)$ in the integrand. Table 2 lists the pertinent information concerning the filters, including the results of the calibrations, which will be described in detail later. It will be noted that filters 2 and 3 (Fig. 4) are both centered at 496.5 nm but that the width of filter 3 is about 1.5 times that of 2. These specifications were chosen for the purpose of investigating the error involved in removing $\Gamma(\lambda)$ from the integral. Without going into detail, we can state that this substitution involved an error of less than 1%. Corroborative evidence is provided

UNCLASSIFIED

Table 2
Filter Characteristics

	LiF(TLD-100)	CaF_2 :Mn	CaF_2 :Mn $CaSO_4$:Mn	$Li_2B_4O_7$:Mn
	Filter 1	Filter 2	Filter 3	Filter 4
Wavelength at mid bandpass λ_0 (nm)	400.3	496.5	496.5	600.5
Transmission at λ_0	0.33	0.59	0.59	0.61
Full width at half maximum (nm)	5.6	6.2	10.3	7.8
R_C*	41.54 ± 0.28%	237.1 ± 0.80%	371.3 ± 0.30%	59.6 ± 0.37%
$\int_\lambda qS_0\, d\lambda$ † (μW/cm²) (By numerical integration)	1.14 ± 6.0%	6.79 ± 6.0%	10.7 ± 6.0%	18.3 ± 6.0%
$M = \frac{\int \varphi\, d\lambda}{\int q\varphi\, d\lambda}$ ‡	57.6	15.9	10.1	16.8

*R_C is the ratio of the response to the standard lamp (during 1 sec) to the response to the light checker.

†The quantity

$$\int_\lambda qS_0\, d\lambda$$

gives the radiant energy flux of the lamp-filter combination at a distance of 43 cm.

‡M is the ratio of radiant energy flux at all wavelengths present in the phosphor spectrum to that passed by the filter.

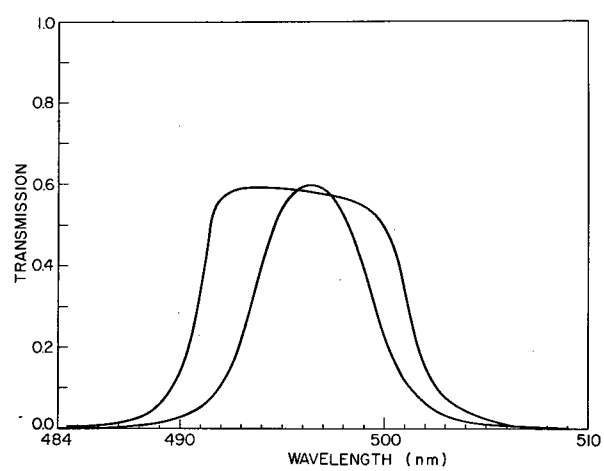

Fig. 4 - Transmission characteristics of broad and narrow 496.5-nm filters. Evidence that the broad filter did not appreciably affect detector characteristics is shown in Fig. 7.

by an examination of Fig. 7. In this plot of the dependence of detected light on mass for CaF_2:Mn the points plotted ○ represent readings taken with the narrow filter, while the Δ points represent those taken with the broad one. It is evident that both sets of points scatter equally about the same line.

There seems little reason to doubt that the filters used with LiF(TLD-100) and $Li_2B_4O_7$:Mn were just as satisfactory as those just described.

Standard Lamp — The standard lamp was a 200-watt iodine-vapor type with a coiled tungsten filament, calibrated by The Eppley Laboratory.* It was used in conjunction with a front-surface mirror specified to be flat to within one-quarter wavelength of the sodium line, furnished with a reflectance curve extending over the visible region.

Because of limited laboratory space the lamp was mounted in a black-velvet-lined box (reflectance about 2%) near the ceiling at one end of the room, the light being brought out through a 3.2-cm-diameter hole at the front of the box. The rear of the box was designed to be a wedge-shaped light trap so that rays traveling antiparallel to the escaping light were reflected at an angle of more than 90 degrees. Air was circulated through the box by means of a small blower.

The mirror, 418 cm from the lamp, was mounted in such a way that it completely shielded its supporting rod from the direct rays of the lamp in an open-ended box. This box was also lined with black velvet and had its back wedge-shaped like that of the lamp box, so that no direct reflection into the path of the incoming and outgoing rays could occur.

The light from the mirror was admitted to the dark box containing the PM tube through a hole cut in the top and fitted with an aperture made of black anodized aluminum. The distance from the mirror to the MgO plaque was 265 cm, and the rays from the mirror were incident on the plaque at an angle of 12 degrees from the normal. During standard-lamp measurements the entire room was totally dark.

The MgO plaque was mounted on a small blackened support furnished with two holes in the bottom surface which mated with studs screwed into the bottom of the box. When glow curves were being run, these studs mated with similar holes in the bottom of the heater strip support. Thus, these two supporting units could be accurately repositioned when one was replaced by the other. The height of the plaque support was designed so that the surface of the plaque was at the same height as the surface of the phosphor within a few tenths of a millimeter. Since the cathode of the PM tube was located vertically about 15 cm above the plaque surface, these variations in height caused errors of no more than a few tenths of a percent. This was confirmed by measurements made with a support of adjustable height.

The MgO plaques were made according to standard procedure by "smoking" a 3.8-cm square of aluminum, which had previously been given a coat of TiO_2 paint, to a thickness of at least 1.3 mm. These were freshly prepared immediately before each calibration run. The desired area of MgO was obtained by placing over the plaque a carbon-blacked mask made of 0.08-mm-thick blued-steel sheet and having a 2.2233 ± 0.0008-cm hole machined in it. With the plaque in place the aperture on the PM tube box was adjusted to fill the hole in the plaque mask with light, slightly overlapping the mask. The error involved due to reflection from the mask was estimated to be less than that caused by variations in height.

*The Eppley Laboratory, Inc., Newport, Rhode Island.

UNCLASSIFIED

Current for the standard lamp was furnished by a Sorenson Model 1000-S voltage regulator (power distortion specified to be less than 0.1%) in order to protect against drift of the power line. The current was monitored by an electrodynometer ammeter, the calibration of which was checked at the NRL Secondary Standards Laboratory to be within 0.25% of full scale. The meter reading was checked just before and just after each exposure of the PM tube to the MgO plaque.

Calibration Procedure — With the required filter and the freshly prepared MgO plaque in place, the optical alignment was carefully checked while the lamp warmed up (at least 5 minutes). Next the sequence of exposures to the light checker and the illuminated plaque were made as already described. After the appropriate corrections for dark current, the ratio R_C of the integrated plaque output to the integrated light-checker output, for equal exposure times of 1 sec, was calculated. The procedure was then repeated, usually about ten times for a calibration.

Calibrations against the light checker were carried out on both the day before and the day after the glow curves for a particular phosphor were run. By using the light checker, the reproducibility of the calibration procedure was checked, i.e., the combined reproducibility of the MgO b[illegible]on, the optical alignment, and the standard lamp current. The calibration of the 400.3-nm filter was repeated several times over a period of 3 months. The resulting R_C value (41.54) listed in Table 2, line 5, is the mean of 51 readings; the coefficient of variance is 0.28%.

Experimental Procedure — The procedures for measuring glow-curve areas (i.e., for integrating PM-tube currents) are given at first only in outline, since the details of handling the phosphors differed somewhat from one phosphor to another and are discussed later. Subsequent to irradiation and any special treatment required, samples were weighed out, starting at about 20 mg, and spread as evenly as possible over the area of the planchet. After light-checker and dark-current measurements were made, the planchet was placed on the heater strip, the shutter was opened, and the heating cycle integrator, and clock were started simultaneously. The glow curve vs time was monitored on the recorder, since any malfunction was indicated by the recorder trace. When the recorder trace showed the glow curve to be complete (e.g., to have returned to the zero-intensity baseline), the clock and integrator were stopped and the heating current switched off. The integrated PM-tube current and the elapsed time were then recorded. The counter was reset to zero, after which the clock was preset to the same elapsed time and an integration of the dark current was performed without closing the shutter. On completion of the dark-current run, the shutter was closed and the light checker was inserted and integrated for 4 minutes as described before. After a sufficient time had elapsed for the heater strip to cool, the process was repeated for the next sample.

Following the usual corrections for dark current the glow-curve areas were divided by the light-checker output per second yielding the quotient R_ϕ. In taking the ratio R_ϕ/R_C the light-checker values cancel out,* leaving the same ratio L as in Eq. 20:

$$L = \frac{R_\phi}{R_C} = \alpha' m G \ . \tag{21}$$

It will be noted that, while R_C is a constant for any given filter, R_ϕ will depend on the mass of the sample. This ratio was taken for each sample in a set of glow curves and the result plotted against mass. The results are the L plots shown in the upper portion

*Since the ratio R_C is independent of time, it is also the ratio of the light-checker and plaque outputs for 1 second.

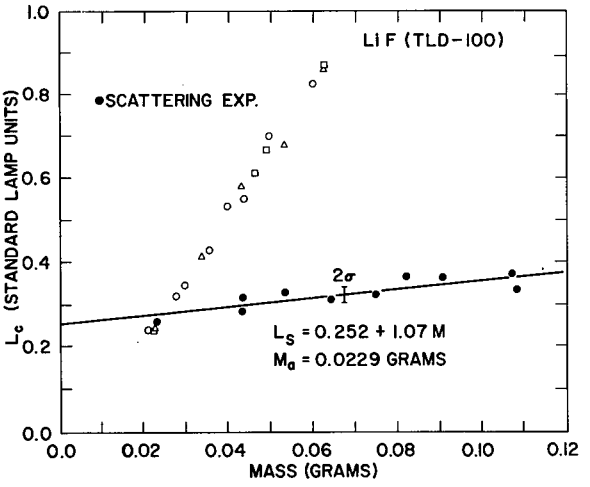

Fig. 5 - Experimental results for LiF(TLD-100). The open points — square, circle, and triangle — give the light collected versus mass of totally active phosphor for three separate aliquots. The filled circles are the results of the scattering experiment and represent the light collected from an active 0.0229-g sample modified by the addition of increasing amounts of unirradiated phosphor.

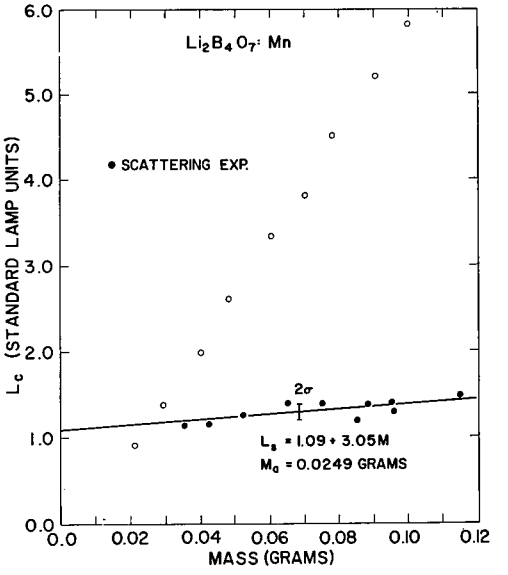

Fig. 6 - Experimental results for $Li_2B_4O_7$:Mn. The open circles represent the light collected versus mass of totally active phosphor. The filled circles show the effect of increasing amounts of inert phosphor on the light collected from an active 0.0249-g sample.

of Figs. 5, 6, 7, and 8. It should be stressed that L represents the light emitted by the phosphor which is passed by the filter and falls on the photocathode and that this is being measured in units of light from the MgO button in 1 second passed by the filter to the photocathode, i.e., in standard lamp unit (SLU). These units are of different magnitude for each filter, but their value in absolute (i.e., energy) units is easily calculated, as will be shown presently.

Variations in Procedure for LiF(TLD-100) (Harshaw Batch 26 EFH) — Two major problems encountered with LiF(TLD-100) in the present context were (a) the sensitivity of its response to the thermal history of the sample and (b) the fading of the low-temperature peaks. Both of these were overcome by rigid adherence to the following annealing schedule: (a) 1 hour at 400°C followed by rapid (about 3 min) cooling to room temperature, (b) 24 hours at 80°C followed by air cooling to room temperature, (c) γ-ray exposure, and (d) postdose anneal of 15 min at 100°C. This last step emptied the remaining traces of the low-temperature peaks at 100° and 150°C. This schedule is the same as that used by Suntharalingam, et al. (11). The data points shown on the L plot, Fig. 5, come from three aliquots which were processed independently.

UNCLASSIFIED

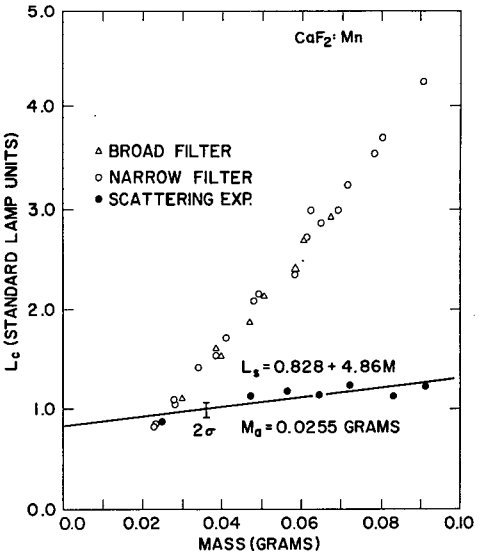

Fig. 7 - Experimental results for CaF_2:Mn. The open points — triangles and circles — represent the light collected versus mass of totally active phosphor for the broad and narrow filters, respectively. The fact that these points are experimentally indistinguishable shows that even the broad filter effectively eliminates the dependence of PM-tube gain on wavelength. The filled circles show the effect of increasing amounts of inert phosphor on the light collected from an active sample of 0.0255 g.

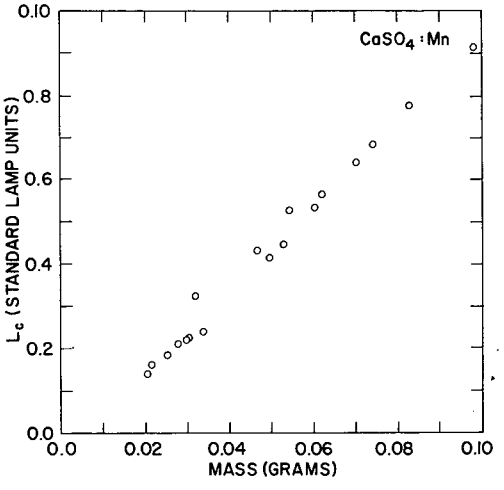

Fig. 8 - Experimental results for $CaSO_4$:Mn. The open circles represent the light collected versus mass of totally active phosphor after a somewhat uncertain correction for fading. No scattering experiment was done with this phosphor.

A minor problem was caused by the appearance of a small higher-temperature peak just before the main peak was finished. It was decided to exclude this minor peak by stopping the integration as soon as the trace started to bend up after completing the main peak (Fig. 3a).

A peculiarity of LiF(TLD-100) is its supralinearity. We were unable to avoid working in the supralinear region, because the large loss of light due to the filters had to be counteracted by increased doses. Hence, the efficiency quoted, 0.062%, is to be listed as that found for an exposure of 5.14 kR. Using response-vs-exposure curves obtained by Marrone and Attix (12) the response for this dose is seen to correspond to about 1.6 times the linear response, from which may be deduced a "low-dose" efficiency of 0.039%.

Variations in Procedure for $Li_2B_4O_7$:Mn (NRL Batch 5X-14) — Of the four phosphors handled, $Li_2B_4O_7$:Mn presented the least difficulty. Heat treatment consisted of a one-half-hour anneal at 300°C followed by a postirradiation anneal of 30 min at 80°C to empty a low-temperature trap at approximately 100°C. Because of the filter losses and the low sensitivity of the PM tube at 600 nm, a 25-kR exposure was required, carrying the

phosphor far into the supralinear region and giving an efficiency of 0.30%. The response curves obtained by West, et al. (13) show this response to be a factor of 4.1 times the extrapolated linear response, leading to a low-dose efficiency of 0.073%.

Variations in Procedure for CaF_2:Mn (E.G. & G., 150-200 mesh, dated April 24, 1967) — The phosphor CaF_2:Mn was annealed at 400°C for 20 min, cooled, and irradiated. Because of the fading, accurately measured by Schulman, et al. (14), which is linear in log t, exposed aliquots were aged for at least 3 days before the samples were glowed out, all on the same day. In this way the same fading correction could be applied to all samples from one aliquot with negligible error. The L data, some of which were taken with the broad (500-nm) filter and some with the narrow one, came from four separate aliquots.

Variations in Procedure for $CaSO_4$:Mn (Prepared by Esther Claffy, NRL) — In addition to the well-known and severe fading problems of $CaSO_4$:Mn, a difficult handling problem was also encountered. As received, the phosphor was in the form of a very small-grained flocculent powder that was impossible to spread evenly in the planchet. This difficulty was finally overcome by placing a sample of the previously irradiated aliquot in the planchet, wetting it with several drops of ethanol, and then gently spreading it with a small camel's hair brush. The planchet was then placed in a bell jar and vacuum dried for at least 30 min, after which it was removed and the glow curves were obtained.

The accuracy of the fading data for this phosphor, Fig. 9, is subject to considerable doubt. Due to unavoidable circumstances the temperature could not be controlled during the 42-min exposure and a like period required for sample preparation. The data have been selected in the sense that several apparently "wild" points (occurring simultaneously in the L-vs-m plot, Fig. 8, and the fading plot) were discarded.

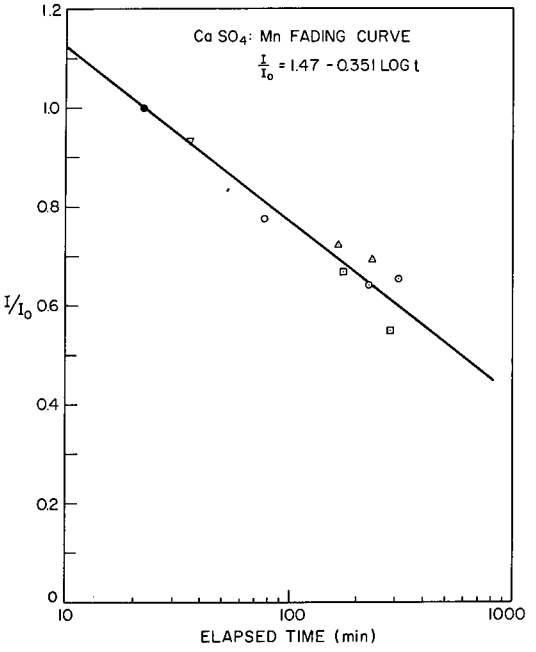

Fig. 9 - The fading curve for $CaSO_4$:Mn. The elapsed time is measured from the beginning of irradiation. The base value (filled circle) was chosen at 21 minutes, which is half the irradiation time. The open points represent data from different aliquots.

UNCLASSIFIED

Data Reduction

The Angular Distribution of Light Intensity — The section on Optics was introduced with a general discussion of Lambertian and non-Lambertian sources. While it is generally recognized that an illuminated MgO plaque is Lambertian, it is not so generally known that thin layers of phosphor, not completely covering the substrate, are not. The following "gedenken experiment" serves to illustrate the argument. Suppose that a plane horizontal circular Lambertian light source is emitting 1 erg/sec into the upper hemisphere only. Vertically above the center of this light source is mounted a detector. The detector, at a distance very large compared with the source diameter, is constrained to move so that the same distance from the source center point is always maintained (i.e., on a concentric hemispherical surface). If the experimenter finds an initial response reading of unity (at $\theta = 0$) and then moves the detector in any direction, he finds that the intensity falls as $\cos\theta$, where the angle θ is subtended at the source between the new position and the vertical. This illustrates Lambert's law of diffuse sources, which predicts that the light intensity will be proportional to the area of the source projected in the direction described by θ. It is qualitatively explained in terms of the fact that the light from the source is scattered away from the $\theta = 90$ degree direction through encounters with source material in the plane of the surface.

We now replace the Lambertian source with an absolutely black planchet of the same dimensions on which a single, very small spherical grain of glowing phosphor is placed. Such a sphere is obviously a 4π (or isotropic) source; i.e., it radiates its light equally into all 4π srad of surrounding space. Suppose that its total emission is also 1 erg/sec. If the experimenter now takes a reading in the vertical direction ($\theta = 0$ degree) he will find the response is 1/4 of that obtained with the Lambertian source (Fig. 10a). One factor of 1/2 results from the one-sided Lambertian source described, emitting only into the upper hemisphere, while the spherical distribution emits equally into the upper and lower hemispheres (even though the bottom half is absorbed by the planchet). The other factor of 1/2 results from the difference in spatial distribution in the upper hemisphere. Whereas for the sphere, the intensity at $\theta = 90$ degrees is the same as in the vertical direction; for the Lambertian source the intensity at 90 degrees is zero. For the Lambertian case we have (from Eq. 3)

$$1 \text{ erg/sec} = 2\pi I_{L_0} \int_0^{\pi/2} \cos\theta \sin\theta \, d\theta$$

and

$$I_{L_0} = \frac{1}{\pi} \text{ erg/srad-sec}$$

For the isotropic case

$$1/2 \text{ erg/sec} = 2\pi I_0 \int_0^{\pi/2} \sin\theta \, d\theta$$

and

$$I_0 = \frac{1}{4\pi} \text{ erg/srad-sec} .$$

A cross-sectional view of the two cases is shown in Fig. 10a.

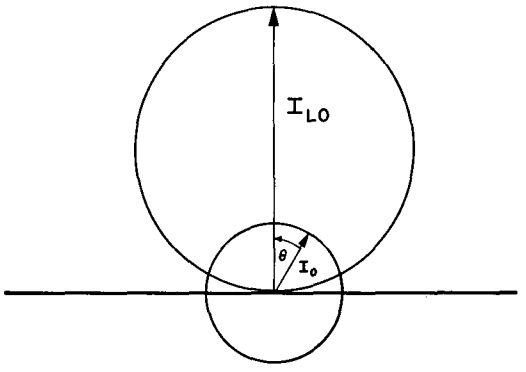

(a) The relative intensities for a Lambertian and an isotropic source emitting the same total energy.

(b) Spatial distribution for an intermediate source. The solid semicircles show the effect of increasing phosphor mass if the sample were always isotropic. The dashed curves show (qualitatively) how both intensity and distribution change with increasing mass.

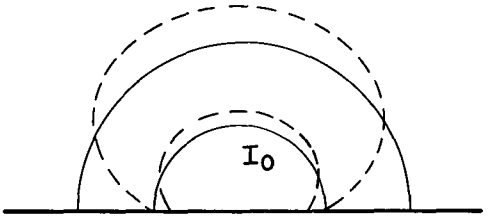

Fig. 10 - Spatial distribution of intensity for Lambertian and isotropic sources.

If now a second identical grain of glowing phosphor is placed on the planchet, the response of the detector at $\theta = 0$ degree will be more than doubled, since it will receive some scattered light from both grains, in addition to the direct light. At the same time the light intensity emitted at $\theta = 90$ degrees, averaged over all directions in the plane of the planchet, will be less than twice that from one grain alone, because one grain will obscure the other when viewed from some directions. It is evident that the addition of many grains progressively increases the $\theta = 0$ degree signal over and above the value it would have from the direct light only, while decreasing the 90-degree signal below its value for direct light. Evidently if this process is carried to the limit, the phosphor will (in the absence of absorption) approach a Lambertian source. In this case, as predicted by Eqs. 3 and 4, the light intensity at $\theta = 0$ degree will be twice as great as that due to direct emission alone. That is, it will consist of half direct light and half scattered light. At $\theta = 90$ degrees the intensity will become nearly zero.

In the case of actual phosphors the light output from a few individual grains is too small for measurement in the present apparatus, so we cannot closely approximate an isotropic source. On the other hand it has been found experimentally that even with thousands of grains we do not approach a Lambertian source. In the next section (Scattering Experiments) it will be shown that, for the smallest samples used, the intensity at $\theta = 0$ degree due to scattered light is only 10 or 15% of the direct light, while for the largest samples used the scattered light was 30 to 50% of the direct light instead of 100% as required for a Lambertian source. Thus, the approach taken was to correct the phosphor light measurements, on the basis of the scattering experiments, to arrive at the direct light output, i.e., reducing the phosphor layer to an isotropic source. This was the basis for the final calculations comparing this output with that from the Lambertian MgO plaque.

It is instructive to predict what the experimenter should observe as the sample mass is increased from very small to larger values. By Eq. 21

UNCLASSIFIED

$$L = \alpha' m G ,$$

where (by Eq. 9)

$$G = \left[2 \int_0^{\pi/2} f(\theta) \sin \theta \, d\theta \right]^{-1}$$

For very small masses the phosphor is a 4π radiator, $f(\theta)$ is unity, and $G = 1/2$. Equation 21 yields

$$L = \frac{1}{2} \alpha' m . \tag{22}$$

For a succession of samples of small but increasing mass a plot of L vs m would yield a straight line with slope $\alpha'/2$ (lower line of Fig. 11).

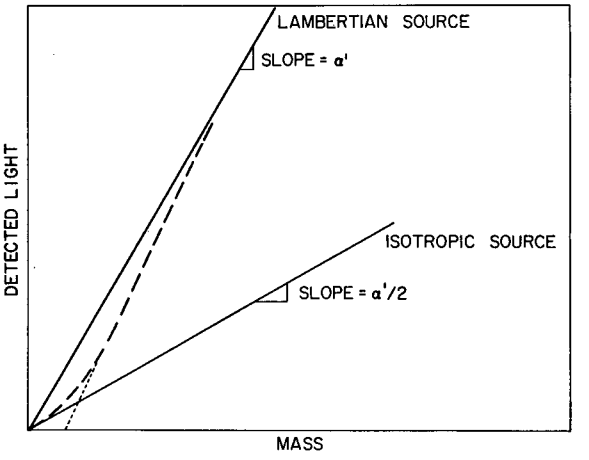

Fig. 11 - Qualitative plot of the increase in detected light with increasing phosphor mass. The dashed line shows the curve to be expected from practical phosphor samples. For intermediate masses the curvature is slight and would be masked by experimental scatter. Linear extrapolation of the data would yield zero light for small but finite masses, as found in the present experiments.

On the other hand, if the phosphor sample were always Lambertian, $f(\theta)$ would be $\cos \theta$ and $G = 1$. Equation 21 would become

$$L = \alpha' m \tag{23}$$

and the L-vs-m plot would yield a straight line with slope α' (upper line of Fig. 11).

In practice L starts out on the $\alpha'/2$ line for very small masses, but with further increases in mass it bends up away from the $\alpha'/2$ line, finally bending over and approaching the α' or Lambertian line for very large masses, as shown by the dashed curve in Fig. 11.

It would be expected that a completely 4π source is obtained for only a few grains (a condition below experimental sensitivity). For a few thousand grains much of the light initially emitted roughly parallel to the plane of the planchet will be scattered into a different direction, so that for values of θ approaching 90 degrees the intensity will be reduced. Since most of the light scattered out of the horizontal plane must appear elsewhere, it will add a component to the intensity normal to the plane. Figure 10b represents a cross section of the spatial distribution described above for two different masses of

phosphor. The plain lines represent the distribution of intensity if the sample were a 4π source. The dotted lines illustrate qualitatively how the isotropic distribution is modified by scattering. If scattering were absent, the spatial distribution of light for successively larger masses would be represented by a succession of concentric hemispheres with radii (corresponding to I_0) simply proportional to mass. A plot of detector response vs mass would give a straight line with slope $\alpha'/2$ and extrapolating to zero for zero mass. Since scattering is present, the distribution is qualitatively like that shown by the dotted curves. The successive intensities seen by the detector are the sums of direct intensities, which are linearly proportional to mass, and scattered intensities, which depend on mass but in an unknown way.

As we have pointed out, it is likely that a truly Lambertian distribution will be attained only for multiple layers of phosphor. In such a case the detector is never exposed directly to the lower lying grains but receives their light only after one or more scattering events, with a consequent increase in absorption by the phosphor. It is well known that, as the thickness of a phosphor layer is increased indefinitely, the light output eventually saturates. This has been reported by Schayes, et al. (4) among others. Hamaker (15) has derived an expression predicting the observed light-output-vs-mass curve for such a case. The differential increase of light with mass is greatest for very small masses, falls monotonically with increasing mass, and approaches zero for very large masses. In simplest terms the effect is due to the enhancement of absorption caused by multiple scattering events. Clearly this does not describe the curve presented in Fig. 11, because his theory is not applicable if the phosphor layer is less than 5 to 10 photon mean free paths (i.e., several grains) in thickness. To stay away from this region we have confined ourselves (except in the case of $CaSO_4$:Mn, where it was unavoidable) to phosphor layers less than one grain thick, where it would be expected that very few photons would be scattered more than a few times and absorption can be neglected. Experimentally the lower limit to the sample mass was set by the sensitivity of the PM tube (in no case were masses of less than 20 milligrams used), and the upper limit was determined by judging when a reasonably good spread in masses had been achieved. Referring to Fig. 11 we see that the dashed curve bends away from the isotropic source line relatively rapidly for low masses and that the curvature decreases with mass. Clearly our data (Figs. 5, 6, and 7) must fall in this region of low curvature. The upper end of the dashed line has not been sketched in, because the onset of appreciable absorption implies that the line of slope α' will never be reached in practice.

Scattering Experiments — To determine the dependency of the scattered component of intensity on mass, experiments were performed in which a fixed amount of irradiated phosphor was mixed with varying amounts of unirradiated phosphor. In terms of the discussion of Fig. 10b, this corresponds to keeping the intensity of direct light constant and measuring the variation of the scattered component. Certainly the light scattered by a particular grain is independent of whether or not the grain itself is emitting light. From Eq. 21 the resultant intensity L_S is given by

$$L_S = \alpha' m_a G \ , \tag{24}$$

where m_a is the fixed mass of irradiated phosphor. The function G (Eq. 9) is not affected. The results are shown plotted against total mass in the lower parts of Figs. 5, 6, and 7. The relatively large scatter arises, at least in part, from the experimental impossibility of maintaining m_a at exactly the same value for each sample. It is apparent that within the limits of experimental accuracy the quantity $\alpha' m_a G$ can be described by a straight line. Accordingly the data were fitted by least squares to equations of the form

$$L_S = C + dm \ , \tag{25}$$

UNCLASSIFIED

where C is the intercept and d the slope of the line. The values so obtained are listed in columns 3 and 4 of Table 3 together with their coefficients of variation. It is evident that the slopes differ significantly from zero in spite of the experimental scatter and that the intercepts are relatively insensitive to scatter.

Table 3
Scattering Corrections

Phosphor	m_a* (g)	C†	d‡	$G(m_a)$§	m_h¶ (g)	$G(m_h)$**	$\frac{d}{m_a}$‡‡
LiF(TLD-100)	0.0229	0.252 ±7.3%	1.07 ±23%	0.548	0.0625	0.633	46.7
$Li_2B_4O_7$:Mn	0.0249	1.09 ±9.4%	3.05 ±45%	0.535	0.110	0.645	123
CaF_2:Mn	0.0255	0.828 ±7.4%	4.86 ±15%	0.575	0.0904	0.765	191
$CaSO_4$:Mn	#	#	#	#	#	#	20

*Average mass of active phosphor used.
†Intercept of the lines fitted to the scattering data.
‡Slope of the lines fitted to the scattering data.
§The calculated values of G for the mass of the active phosphor.
¶The largest total sample mass used in obtaining the L_C curves.
**The calculated values of G for the largest total sample mass.
††The coefficient of the mass-squared term (Eq. 33) used to correct to an isotropic source.
#No scattering experiments were done with $CaSO_4$:Mn.

Clearly C represents the extrapolation to zero mass of Eq. 24. Since it has been seen that the limiting value of G for small masses is 0.5, it follows that

$$0.5\ \alpha' m_a = C\ . \tag{26}$$

On the other hand for any mass m within the experimental range, it follows from Eq. 24 that

$$\alpha' m_a G(m) = L_S(m)\ . \tag{27}$$

Taking the ratio of Eqs. 27 and 26 and solving for $G(m)$ yields

$$G(m) = 0.5\,\frac{L_S(m)}{C} = 0.5\,\frac{(C + dm)}{C}\ . \tag{28}$$

It is instructive to calculate, using Eq. 28, the values of G for the values of m_a, representing the smallest masses used in the scattering experiments. The results are listed in column 5 of Table 3, where it is seen that the $G(m_a)$ values differ from 0.5, the zero-mass value, by 15% in the case of CaF_2:Mn and about 10% for the other two phosphors. Thus, the extrapolation to zero mass does not represent a large excursion from experimental values and so may be used with some confidence.

It is also useful to consider the G values for m_h, the largest masses used in the L-vs-m plots. These are listed in column 7 of Table 3. It is immediately apparent that these differ from 1 (the value of G for a Lambertian source) by much larger amounts than the G values for m_a differ from 0.5. In other words, in the course of this experiment the phosphor-covered planchet never approached being Lambertian, while for the smaller masses it was within 15% of being an isotropic source.

Calculations — From the foregoing discussion it is clear that the best approach for evaluating α' from the experimental data is to estimate the amount by which the phosphor samples deviate from an isotropic source and apply these deviations as corrections to the experimental data. The result will be a line of slope $\alpha'/2$ from which α' may easily be found

For this approach it is convenient to make a change in notation by setting

$$G(m) = \frac{1}{2} + gm \ , \tag{29}$$

where g is a constant. Thus, Eq. 21 becomes

$$L_C = \alpha' m \left(\frac{1}{2} + gm\right)$$

$$= \frac{1}{2}\alpha' m + \alpha' g m^2 \ . \tag{30}$$

Equation 25 now becomes

$$L_S = C + dm = \frac{1}{2}\alpha' m_a + \alpha' m_a g m \ . \tag{31}$$

Evidently

$$\alpha' m_a g = d$$

and

$$\alpha' g = d/m_a \ . \tag{32}$$

Substituting Eq. 32 into Eq. 30 and solving for $\alpha' m/2$, the result is

$$L_{4\pi} = \alpha' m/2 = L_C(m) - \left(\frac{d}{m_a}\right) m^2 \ . \tag{33}$$

Thus, the value of each sample represented by $L_C(m)$ was corrected by an amount given by the product of the factor d/m_a (listed in column 8 of Table 3) and the square of its mass. The results are plotted in Figs. 12, 13, 14, and 15. These plots were then fitted by least squares to a straight line with a zero intercept. The slopes, which are labeled $\alpha'/2$ are shown in the second column of Table 4.

Because of conditions over which we had no control, it was not possible to do a scattering experiment with the $CaSO_4$:Mn phosphor. Since the L_C plot of this phosphor resembled that of the others, a correction proportional to the square of the mass was also applied to this phosphor. The proportionality factor (column 8, Table 3) was found through trial and error as that which resulted in an $L_{4\pi}$ plot with a zero intercept.

UNCLASSIFIED

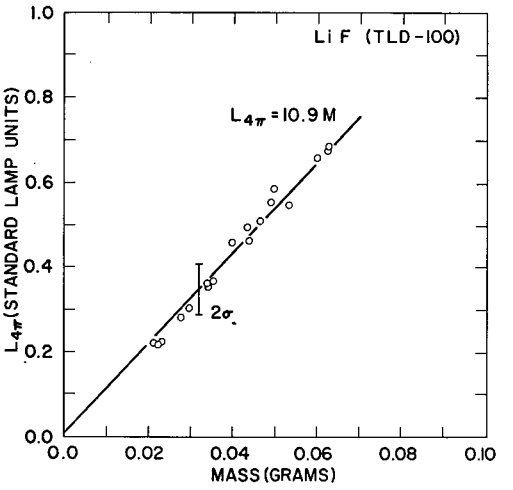

Fig. 12 - Results corrected for scattering: LiF(TLD-100)

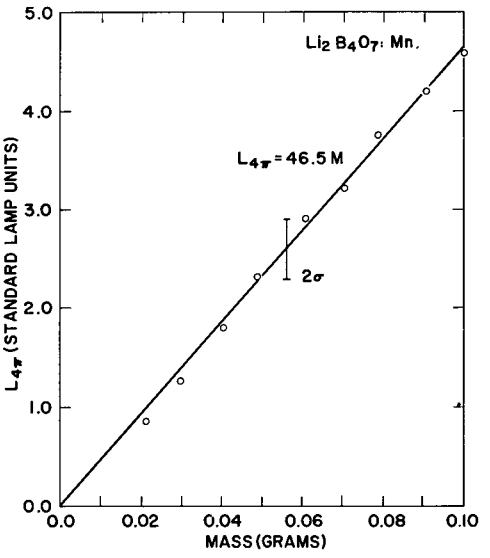

Fig. 13 - Results corrected for scattering: $Li_2B_4O_7$:Mn

It remains to make the correction for the reflectivity of the planchet. For zero reflectivity the energy in the upper hemisphere would be half the total energy $\mathcal{E}_\phi$ emitted by the phosphor; however, since the planchet reflects 0.07 of the light falling on it (which would otherwise be radiated into the lower hemisphere), the actual value of E_ϕ is

$$E_\phi = \frac{1}{2}\mathcal{E}_\phi + 0.07 \times \frac{1}{2}\mathcal{E}_\phi .$$

Recalling, by Eq. 15, that E_ϕ in SLU is given by $\alpha' m$ it follows that

$$\alpha' m = \left(\frac{1.07}{2}\right)\mathcal{E}_\phi = \left(\frac{1.07}{2}\right)\alpha m$$

and

$$\alpha' = 0.535\,\alpha . \tag{34}$$

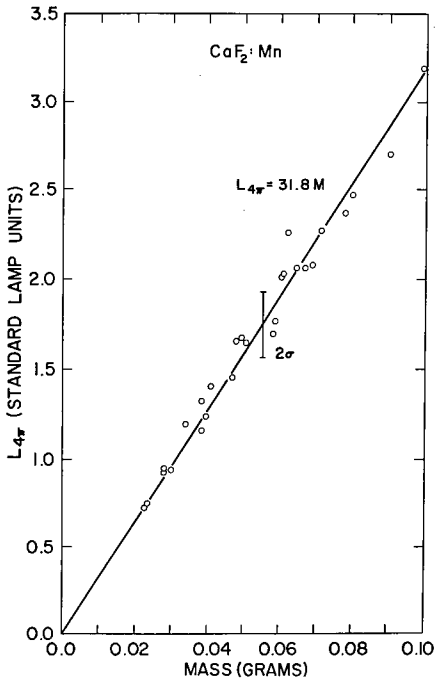

Fig. 14 - Results corrected for scattering: $CaSO_2$:Mn

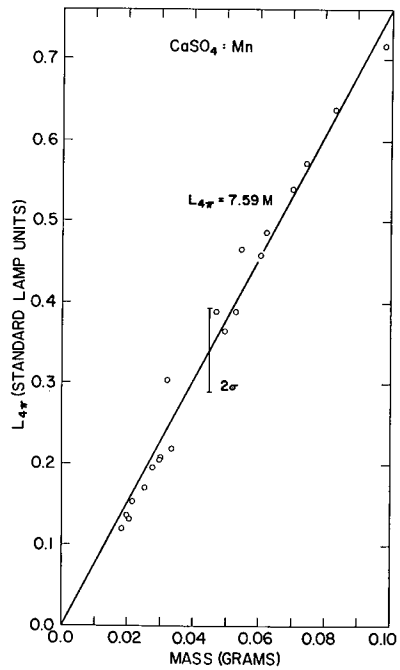

Fig. 15 - Results corrected for scattering: $CaSO_4$:Mn. In this case the scattering coefficient was found by trial and error (see text).

UNCLASSIFIED

Table 4
Relative Light Output Per Unit Mass

Phosphor	$\alpha'/2$*	α' †	α ‡
LiF(TLD-100)	10.9 ± 1.1 (σ = 0.061)	21.8 ± 2.2	40.8 ± 4.3
$Li_2B_4O_7$:Mn	46.5 ± 4.1 (σ = 0.31)	93.0 ± 8.2	174 ± 16
CaF_2 :Mn	31.8 ± 1.7 (σ = 0.18)	63.6 ± 3.4	118.9 ± 7.5
$CaSO_4$:Mn	7.59 ± 1.9 (σ = 0.053)	15.2 ± 3.8	28.4 ± 7.2

*This column gives the slopes of the $L_{4\pi}$ curves along with the standard error and the scatter about the fitted line (the uncertainty in the value for $CaSO_4$:Mn was taken as 25%).

†The factor α' represents the calculated slopes for an equivalent Lambertian source.

‡The quantity α gives the total light emitted by the phosphor per gram in both the upper and lower hemispheres; it includes a correction for the reflectivity of the planchet. The value for the $CaSO_4$:Mn was selected to give a zero extrapolation to the corrected data.

Table 4 lists the best values of α (together with the corresponding uncertainties) as calculated from α' and Eq. 34.

It will be recalled that all calculations to this point have been based on the light transmitted by the filter. If α_t is defined as the energy emitted (SLU/g) for all wavelengths in the phosphor spectrum, then clearly

$$\frac{\alpha_t}{\alpha} = \frac{\int_\lambda \Phi(\lambda)\, d(\lambda)}{\int_\lambda \Phi(\lambda)\, q(\lambda)\, d\lambda}. \tag{35}$$

Defining the ratio of the two integrals as M, it is clear that α_t is given by the product $M\alpha$.

To find M, expanded-scale plots of Gorbics' (6) spectra and the filter characteristics were constructed. Here a difficulty was encountered; because of the lack of instrumental sensitivity the limits of Gorbics' spectral distribution curves in no case extended beyond an intensity which was a few percent of the maximum. His LiF(TLD-100) spectrum does not extend above 500 nm, at which point the intensity is about 30% of the maximum. In the case of the $Li_2B_4O_7$:Mn spectrum the lack of sensitivity in the red precluded measurement of intensities below about 80% of the maximum on the long wavelength side of the curve. Except for the latter case the curves were extrapolated linearly to zero; for the $Li_2B_4O_7$:Mn the curve was assumed to be symmetrical about its maximum and its area was taken to be twice that of the short wavelength side.

Integration was performed numerically: The results are listed in Table 5 along with the estimates of M and the computed values of α_t. The area contributed by the extrapolations and the estimated errors therefrom are also given. The two values of α_t for CaF_2:Mn are not in conflict. It should be remembered that they are expressed in SLU's, which are of different magnitude.

Table 5
Phosphor Spectra and Derived Values

Phosphor	$\int \varphi \, d\lambda$ (arbitrary units)	Fraction of $\int \varphi \, d\lambda$ Contributed by Extrapolated Area (%)	$\int q\varphi \, d\lambda$ (arbitrary units)	$M \left(= \frac{\int \varphi \, d\lambda}{\int q\varphi \, d\lambda} \right)$ (dimensionless)	$\alpha_t (= M\alpha)$* (SLU/g)
LiF(TLD-100)	123.2 ± 8.2	7.8 ± 3.9	2.14 ± 0.14	57.6 ± 5.3	2350 ± 330
$Li_2B_4O_7$:Mn	87.9 ± 13.0	28 ± 14	5.23 ± 0.33	16.8 ± 2.7	2920 ± 540
CaF_2:Mn Narrow filter	63.2 ± 3.7	0.85 ± 0.43	3.98 ± 0.25	15.9 ± 1.4	1890 ± 190
Broad filter	63.2 ± 3.7	0.85 ± 0.43	6.28 ± 0.40	10.06 ± 0.87	1200 ± 130
$CaSO_4$:Mn (Broad filter)	70.9 ± 4.1	2.5 ± 1.3	6.27 ± 0.40	11.29 ± 0.97	304 ± 80

*The factor α_t gives the calculated values of light emitted at all wavelengths per gram of phosphor.

Evaluation of the Standard Lamp Units — The standard lamp unit, it will be recalled, is the light energy diffusely reflected by the MgO button which will be passed by the filter in 1 second. It is calculated by

$$1 \text{ SLU} = 1 \text{ sec} \times \left(\int q S_0 \, d\lambda \ \mu\text{W/cm}^2\right) \times (10 \text{ erg}/\mu\text{W-sec})$$

$$\times \left(\frac{d_0}{d}\right)^2 \times [A_B \cos\theta \text{ cm}^2] \times R_M(\lambda_0) \times R_{MgO}(\lambda_0) \ , \tag{36}$$

where

$\int qS_0 \, d\lambda$ = the intensity, at the distance of its calibration (d_0), of the light emitted by the lamp which will be passed by the filter

10 erg/μW-sec = the conversion factor of μW-sec to erg

$\left(\frac{d_0}{d}\right)^2$ = $(43/681.5)^2$ = the squared ratio of the distance of the lamp calibration to the distance from the lamp to the plaque

$A_B \cos\theta$ = (3.882 × 0.845) the area of the plaque projected normal to the incident light

$R_M(\lambda_0)$ = reflectivity of the mirror at the center of the filter band

$R_{MgO}(\lambda_0)$ = reflectivity of the MgO at the center of the filter band

UNCLASSIFIED

The product of the geometric factors $(d_0/d)^2$ and $A_B \cos \theta$ is the same for all filters and is calculated to be 0.01310 ± 0.00011 cm^2. Combining this product with the unit of time and the conversion of μW to erg/sec factor gives 0.1310 ± 0.0011 $erg^2/\mu W$, which is common to the calculation of all SLU.

Table 6 lists the filter dependent factors of the standard lamp calibration. The term $\int qS_0 \, d\lambda$ was determined by numerical integration of the filter characteristics and standard lamp spectrum. The term $R_M(\lambda_0)$ was taken from the reflectance curve of the mirror, and the $R_{MgO}(\lambda_0)$ term was taken from the values for the reflectance of MgO given in the Handbook of Chemistry and Physics (16).

Table 6
Absolute Values of the Standard Lamp Units (SLU)

Wavelength (nm)	$\int_\lambda qS_0 \, d\lambda$* ($\mu$W-sec/$cm^2$)	$R_M(\lambda_0)$†	$R_{MgO}(\lambda_0)$‡	1 SLU (= E_L ergs)
400	1.140 ± 0.073	0.751 ± 0.015	0.97 ± 0.02	0.1088 ± 0.0077
500 (Narrow)	6.79 ± 0.43	0.894 ± 0.018	0.98 ± 0.02	0.779 ± 0.055
500 (Broad)	10.70 ± 0.68	0.894 ± 0.018	0.98 ± 0.02	1.228 ± 0.087
600	18.3 ± 1.2	0.929 ± 0.019	0.98 ± 0.02	2.18 ± 0.15

*The $\int_\lambda qS_0 \, d\lambda$ values are carried over from Table 2, line 5.
† $R_M(\lambda_0)$ represents the reflectance values for the mirror at the wavelength in question.
‡ $R_{MgO}(\lambda_0)$ represents the reflectance values for MgO at the wavelength in question.

RESULTS

Calculation of Efficiencies

The total light emitted per gram of phosphor α_t in ergs can now be determined, since the absolute value of the SLU is known in each case. The ratio of this number to the energy absorbed per gram during irradiation gives the efficiency, which is the number sought. For convenience these values are listed in Table 7.

Relative Efficiency

Before intercomparing these efficiencies, it should be noted that both of the lithium-based phosphors have been dosed well into the supralinear region. For LiF(TLD-100) this gives an enhancement of response of about 1.6 above linear. For $Li_2B_4O_7$:Mn the enhancement is by a factor of 4.1. Table 8 lists the low-dose efficiencies together with their values relative to that of LiF(TLD-100). It is of interest to note that the efficiencies of the lithium-based phosphors are nearly equal and that the calcium-based phosphors are an order of magnitude higher. Another quantity of interest is the light output per gram per R exposure for low doses. This value is listed in the last column.

Table 7
Calculated Efficiencies

Phosphor	α_t* (ergs/g)	Energy Absorbed (ergs/g)	Intrinsic Efficiency η (%)	Probable Error (%)
LiF(TLD-100)	255 ± 40	$(4.15 \pm 0.21)\times 10^5$	0.062†	17
$Li_2B_4O_7$:Mn	6400 ± 1300	$(2.12 \pm 0.11)\times 10^6$	0.300‡	21
CaF_2:Mn				
Narrow filter	1470 ± 190	$(3.38 \pm 0.17)\times 10^5$	0.436	14
Broad filter	1470 ± 190	$(3.38 \pm 0.17)\times 10^5$		
$CaSO_4$:Mn (Broad filter)	370 ± 100	$(3.13 \pm 0.14)\times 10^4$	1.19	28

*α_t = energy emitted.
†This value was determined for an exposure of 5.14 kR.
‡This value was determined for an exposure of 25 kR.

Table 8
Low-Exposure Efficiencies, Relative Efficiencies, and Light Output

Phosphor	Efficiency (%)	Efficiency Relative to LiF(TLD-100)	Light Output (ergs/g R)
LiF(TLD-100)* (Linear region)	0.039	1	3.1×10^{-2}
$Li_2B_4O_7$:Mn* (Linear region)	0.0732	1.9	6.2×10^{-2}
CaF_2:Mn	0.436	11	37×10^{-2}
$CaSO_4$:Mn	1.19	31	100×10^{-2}

*Data on these two phosphors have been corrected for supralinearity.

Discussion

Prior to the commencement of this work the author was aware of only four reports (1-4) of efficiency measurements on the phosphors investigated. Since then, an additional report (17) and the work of A.M. Strash* have appeared. Table 9 compares the results.

Where possible the data of the other investigators have been used to calculate efficiency in percent on the same basis as that used in the present report. However, it was not possible to do so with the data presented by Arkhangel'skaya and Razumova (1); their results were given as the ratio of light quanta emitted per γ-ray quantum absorbed, so the present data have been recast in the same form, quantum efficiency. In comparison

*A.M. Strash, private communication.

UNCLASSIFIED

Table 9
Comparison of Efficiency Results

Reference	Efficiency (%)		
	LiF(TLD-100)	CaF_2:Mn	$CaSO_4$:Mn*
Arkhangel'skaya and Razumova	–	–	7.5×10^4†
Bjärngard	–	–	1.5
Morehead‡ (high dose) Stated	0.005	–	–
Corrected	0.0024	–	–
Schayes, et al.	0.072	1.3	–
Strash	0.13	–	–
Present Work Supralinear	0.062	–	–
Linear	0.039	0.44	1.2
Quantum Efficiency	–	–	61×10^4†

*The reason for including the quantum efficiency for $CaSO_4$:Mn is explained in the text.
†The efficiency is given in the form of quantum efficiency.
‡Morehead's stated value of 0.005% is demonstrably in error; therefore, a corrected value is listed.

to the present results, Arkhangel'skaya and Razumova's (1) data for $CaSO_4$:Mn are about a factor of 8 smaller.

On the other hand, Bjärngard's (2) result for this phosphor is within one standard deviation of the result in this report. He also was aware that the light output increases more than linearly with mass, though he attributed the effect to a change in the "apparent reflectivity" of the planchet. He solved the problem by confining his measurements to extremely thin samples which give a very nearly isotropic distribution of light in space. Hence, his assumption of 4π geometry resulted in little error.

However, Bjärngard neglected the reflectivity of his planchet made of Kanthol, which has a medium gray color. In preparation for the investigation reported here, comparative runs were made using aluminum and graphite planchets. It was found that the light from the aluminum planchets was about 1.6 times that from the graphite ones. Since these aluminum planchets had been heated in air repeatedly, they were no longer bright. The experiment demonstrated the importance of planchet reflectivity for thin samples. It is considered quite probable that Bjärngard's efficiency would scarcely differ from the presently reported value if planchet reflectivity had been included; it is easily estimated that a 25% reflectivity for his Kanthol would give exact agreement.

Turning to LiF(TLD-100), it should be stated that Morehead's (3) measurements made in 1951 were almost certainly made on material different from that used in this work. His stated efficiency is 0.005%. However (as pointed out by Attix (5)), there is an error by a factor of nearly two in his calculation of energy absorbed; the correct figure should be 0.0024%. By taking into consideration that Morehead's exposure was given as 325 kR, his corrected figure of 0.0024% is still more than an order of magnitude smaller than the supralinear figure obtained in the present work for LiF(TLD-100) in Table 9.

Schayes, et al. (4) have compared the efficiencies of several phosphors, two of which (LiF(TLD-100) and CaF_2:Mn) were included in the present work. To deduce absolute efficiencies from their data, the quantum efficiency of the photocathode of their PM tube must be accurately known. Since he did not supply this information, the nominal specifications given by the manufacturer were used to calculate the values listed in Table 9. Considering the uncertainties involved, the agreement is not bad. On the other hand, it is to be noted that their results are higher than those reported here in both cases. It is believed that their higher values can be accounted for, at least in part, by their assumption that the phosphor is an isotropic (4π) emitter. However, the fact that their samples were glazed in a binder means that the distribution of light in space is probably not the same as that demonstrated in the present report for loose powder samples. It is also to be noted that they make no mention of the reflectivity of the planchet; such reflection would also cause an overestimate of the light output.

The efficiency of LiF(TLD-100) was most recently measured by A.M. Strash as part of an impressive study of spectral efficiency (18). His measurements were carried out on samples from the same batch used in the present investigation. These samples were irradiated by us to a dose of 500 rad under identical conditions to those reported here. At this level supralinearity is not important, so his number is to be compared with the reported value of 0.04%. It is believed that the factor-of-three difference can be accounted for by (a) his neglect of planchet reflectivity and (b) the erroneous assumption of 4π geometry for his source.

Strash's planchet was silver, which has a high reflectivity and tarnishes very little with repeated use as a planchet (19). The roughness of the surface of his planchet had very little effect since diffuse light reflects diffusely. Our results, referred to above, with aluminum indicate that the reflectivity of silver could easily cause his results to be too large by a factor of 1.6.

The magnitude of error attributable to Strash's assumption of 4π geometry is difficult to assess, since it depends quantitatively on how much his samples deviate from isotropy. In the present work, the largest sample thickness used was 15 mg/cm^2, which gives a detected intensity of about 1.5 times that from an isotropic source of the same total mass (60 m). Strash's samples had a thickness of 38 mg/cm^2 and were spread in oblong planchets having a length-to-breadth ratio greater than 4 to 1. This combination of greater sample thickness and odd planchet geometry makes impossible a reliable estimate of the deviation from isotropy and the resulting error. It is worth noting however that, had the samples in the present work been perfectly Lambertian but assumed to be isotropic, the results would have been larger by a factor of 2. It would not be surprising therefore if Strash's error approached this value.

Another possible source of error in Strash's work should also be pointed out. His Fig. 4 shows that the planchet was located at the bottom of a "well" formed by an aluminum plate and the monochromator mounting plate. Nothing is said concerning the well surfaces, but unless they were thoroughly blackened they could reflect appreciable additional light into the monochrometor causing too high a value for the measured efficiency.

UNCLASSIFIED

ACKNOWLEDGMENTS

The author would like to express his sincere thanks to F. H. Attix for his advice and encouragement in the course of this work, to S. G. Gorbics and A. E. Nash for many stimulating discussions, and to S. Podgor for his able assistance in the computation of least-square fits to the experimental data.

REFERENCES

1. Arkhangel'skaya, V.A., and Razumova, T.K., Krantovyy vykhod termolyuminestsentsii fosfora $CaSO_4$:Mn oblasti 113-0.0048Å; Opt. i Spektroskopiya, Sbornik statey. Tom I: Lyuminestsentsiya, Ed. by S.E. Frish, Academy of Sciences, USSR, pp. 299-305, 1963

2. Bjärngard, B., "The Properties of $CaSO_4$:Mn Thermoluminescence Dosimeters," Aktiebolaget Atomenergi, Report AE-109, Stockholm, Sweden, 1963

3. Morehead, F., Jr., "The Storage of Radioactive Energy in Artificial Crystals and Minerals," Thesis, U. of Wisconsin, 1951

4. Schayes, R., Brook, C., Kozlowitz, I., and Lheureux, M., "Luminescent Dosimetry," AEC CONF-650637, pp. 138-157, 1967

5. Attix, F.H., Health Phys. 15:49 (1968)

6. Gorbics, S.G., "Luminescence Dosimetry," AEC CONF-650637, pp. 167-182, 1967

7. Nash, A.E., and Kunz, W.E., "A Standard Source of Radiation for Radiac Detectors, Part II," NRL Report 5462, Apr. 22, 1960

8. Ritz, V.H., and Attix, F.H., Radiation Res. 16:401 (1962)

9. Attix, F.H., and Roesch, W.C., editors, Chapter 3 in "Radiation Dosimetry," 2nd Edition, Volume I, New York:Academic Press, 1968

10. Gorbics, S.G., Nash, A.E., and Attix, F.H., Intern. J. Appl. Radiation Isotopes 20:829 (Part I) (1969); Intern. J. Appl. Radiation Isotopes 20:843 (Part II) (1969)

11. Suntharalingam, N., Cameron, J.R., Shuttleworth, E., West, M., and Fowler, J.F., Phys. Med. Biol. 13:97 (1968)

12. Marrone, M.J., and Attix, F.H., Health Phys. 10:431 (1964)

13. West, E.J., Nash, A.E., Attix, F.H., Kirk, R.D., and Schulman, J.H., "Thermoluminescent Dosimeters of Lithium Borate," Report of NRL Progress, pp. 1-6, June 1967

14. Schulman, J.H., Ginther, R.J., Gorbics, S.G., Nash, A.E., West, E.J., and Attix, F.H., Intern. J. Appl. Radiation Isotopes 20:523 (1969)

15. Hamaker, H.C., Philips Res. Rept. 2:55 (1947)

16. Handbook of Chemistry and Physics, 44th Edition, 1962-1963

17. Spurný, Z.D., Phys. Med. Biol. 13:465 (1968)

    In a Letter to the Editor Spurný gives the relative sensitivities of several phosphors as computed from his own measurements and data taken from the literature. The only phosphor reported by him which was measured in the present work is

UNCLASSIFIED

Schulman's CaF_2:Mn. However, Spurný's data for this phosphor came from the work of Schayes, et al., which we have cited as Ref. 4.

18. Strash, A.M., "The Thermoluminescence Spectrum and the Energy Convulsion Efficiency of Lithium Fluoride," U.S. Atomic Energy Commission Report HASL-219 (Available from: Clearinghouse for Federal Scientific and Technical Information, National Bureau of Standards, U.S. Dept. of Commerce, Springfield, Va., 22151)

19. Gorbics, S.G., private communication

Appendix A

JUSTIFICATION FOR EXPRESSING THE SOURCE INTENSITY WATTS/STERADIAN INSTEAD OF WATTS/CM^2

To express the source intensity in watts/steradian instead of watts/cm^2 it must be shown that the lateral extension of the source has negligible effect on the light flux as measured at any point on the surface of an imaginary hemisphere of 15-cm radius centered at the center of the planchet of 1.11-cm radius. First, expressing the normal intensity of an element of area da of the source as ξ_0 watts/cm^2 and, assuming that ξ_0 is not a function of position on the surface, integrate over the surface area to find the $\int_0 F\, dA$ incident on an arbitrary element of area dA of the hemisphere. Referring to Fig. A1 the resulting expression is

$$\int_0 F\, dA = \left[\xi_0 \int_0^R \int_0^{2\pi} \frac{(\rho \cos \beta)(\rho \cos \gamma)\, d\phi}{x^2}\right] dA \,, \tag{A1}$$

where ρ, ϕ are the polar coordinates of the element of source area $\rho\, d\phi\, d\rho$, x is the line connecting da and dA, β is the angle between x and the normal to the source, and γ is the angle between x and the normal to dA. Expressing β, γ, and x as functions of ρ and ϕ, Eq. A1 becomes, after some labor,

$$\int_0 F\, dA = \xi_0 \frac{\pi R^2 \cos \theta}{S^2} \psi(\theta)\, dA \,, \tag{A2}$$

where

$$\psi(\theta) = \left[\left(\frac{R}{S}\right)^4 + 2\left(\frac{R}{S}\right)^2 (1 - 2 \sin^2\theta) + 1\right]^{-1/2} \tag{A3}$$

It is easily demonstrated that, for the given values of R and S (1.11 cm and 15 cm, respectively), $\psi(\theta)$ deviates from unity by no more than ±0.6%, which is certainly negligible when compared with experimental error.

To find the total flux incident on the hemisphere, dA is expressed as

$$dA = S^2 \sin \theta\, d\theta d\phi \,.$$

Since all the other quantities in Eq. (A2) are independent of ϕ, it may be integrated over ϕ at once

$$\int_0 A = 2\pi S^2 \sin \theta\, d\theta \,.$$

Thus,

UNCLASSIFIED

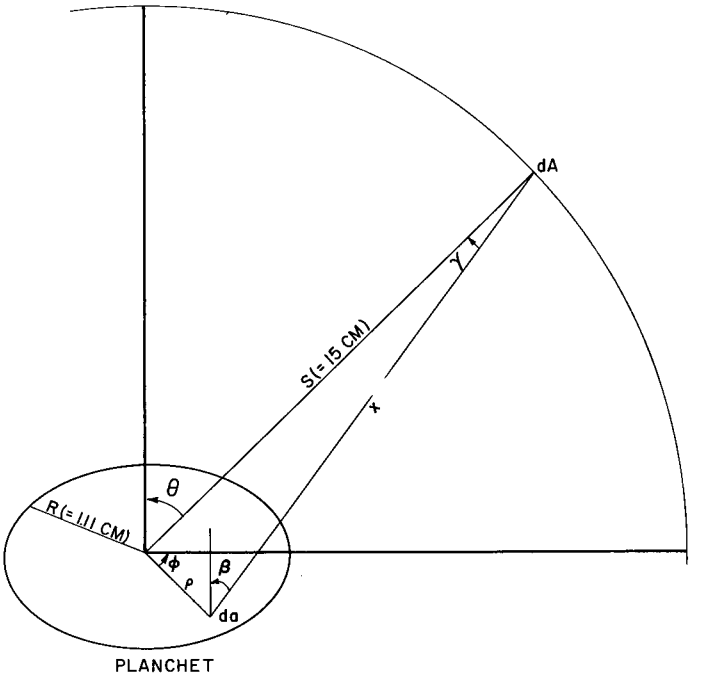

Fig. A1 - Geometry on which Eq. A1 is based

$$F = 2\pi\xi_0(\pi R^2)\int_0^{\pi/2} \psi(\theta) \cos\theta \sin\theta \, d\theta ,$$

so that rigorously

$$F = \pi\xi_0(\pi R^2) \tag{A4}$$

It will be noted that if the same procedure is followed except that $\psi(\theta)$ is set equal to unity before integration exactly the same result is obtained. Hence, Eq. (A2) may be written

$$\delta F)_{dA} = \xi_0 \pi R^2 \cos\theta \, 2\pi \sin\theta \, d\theta$$

Clearly $\xi_0 \pi R^2$ is the total flux normal to the source, which may be written I_0, and $2\pi \sin\theta \, d\theta$ is the element of solid angle $d\omega$. Thus,

$$\delta F)_{dA} = I_0 \cos\theta \, d\omega , \tag{A5}$$

where now I_0 has the units watts per steradian.

The lengthy proof for an <u>isotropic</u> source that

$$\delta F)_{dA} = I_0 \, d\omega \, , \tag{A6}$$

will not be attempted since it is easily shown on a worst-case basis (values of θ near 90°) that the error involved in Eq. A6 is less than that of Eq. A5.

UNCLASSIFIED

Appendix B

PROOF THAT THE RATIO OF DETECTED FLUX TO INTENSITY IS THE SAME (TO WITHIN NEGLIGIBLE ERROR) FOR BOTH LAMBERTIAN AND ISOTROPIC SOURCES

In the section on Optics in the body of the report it was stated that for a Lambertian source the flux F_{L_c} (ergs/sec) falling on the photocathode is given by

$$F_{L_c} = 2\pi I_{L_0} \int_0^{\theta_c} \cos\theta \sin\theta \, d\theta \tag{B1}$$

and for a non-Lambertian source

$$F_c = 2\pi I_0 \int_0^{\theta_c} f(\theta) \sin\theta \, d\theta \ , \tag{B2}$$

where θ_c is the angle between the extreme edge of the photocathode (assumed to be circular) and the central normal to the source. As previously stated, the photocathode was a rectangle with nominal dimensions 0.95 cm × 2.5 cm rather than circular. The proof is constructed on a worst-case basis. Clearly the greater the lateral extent of the cathode the greater the difference in intercepted flux caused by the different source characteristics; therefore, the assumption is made that the cathode is circular with a diameter of 2.5 cm. Since the photocathode is 15 cm from the source

$$\theta_c = \tan^{-1} \frac{1.25}{15} \ .$$

Evaluating Eq. B1, the result is

$$F_{L_c} = 0.006897\pi I_{L_0} \ . \tag{B3}$$

In the body of the report it has been described how the phosphor sample changes from an isotropic source toward a Lambertian one. The worst disagreement is found when, for small masses, the phosphor gives an isotropic source. In this case $f(\theta)$ is unity, and Eq. B2 becomes

$$F_c = 2\pi I_0 \int_0^{\theta_c} \sin\theta \, d\theta \ .$$

Evaluating the integral, Eq. B2 becomes

$$F_c = 0.006908\pi I_0 . \tag{B4}$$

The numerical coefficients in Eqs. B3 and B4 differ by less than 0.2%, which is negligible.

This small difference shows that the variation in intensity with angle is, in the worst case, negligible over the area of the photocathode. Thus the intercepted flux may be calculated by multiplying the normal intensity by the solid angle ω_c subtended by the cathode from a distance of 15 cm. Thus, $\omega_c = 0.0156$, and the quantity c defined in connection with Eq. 6 has the value 0.00336.

Security Classification

UNCLASSIFIED

DOCUMENT CONTROL DATA - R & D

(Security classification of title, body of abstract and indexing annotation must be entered when the overall report is classified)

1. ORIGINATING ACTIVITY *(Corporate author)*

Naval Research Laboratory
Washington, D.C. 20390

2a. REPORT SECURITY CLASSIFICATION

Unclassified

2b. GROUP

3. REPORT TITLE

INTRINSIC EFFICIENCY OF THERMOLUMINESCENT DOSIMETRY PHOSPHORS

4. DESCRIPTIVE NOTES *(Type of report and inclusive dates)*

This is the final report on this problem.

5. AUTHOR(S) *(First name, middle initial, last name)*

William H. Lucke

6. REPORT DATE

August 13, 1970

7a. TOTAL NO. OF PAGES

42

7b. NO. OF REFS

19

8a. CONTRACT OR GRANT NO.

NRL Problem H01-24

b. PROJECT NO.

RR 002-06-41-5009

c. AEC (AT-49-7)-1864

d.

9a. ORIGINATOR'S REPORT NUMBER(S)

9b. OTHER REPORT NO(S) *(Any other numbers that may be assigned this report)*

10. DISTRIBUTION STATEMENT

This document has been approved for public release and sale; its distribution is unlimited.

11. SUPPLEMENTARY NOTES

12. SPONSORING MILITARY ACTIVITY

Department of the Navy (Office of Naval Research) and U.S. Atomic Energy Commission, Washington, D.C.

13. ABSTRACT

The intrinsic efficiency is defined as the ratio of light energy emitted during heating to energy absorbed during gamma irradiation. This factor was measured for four commonly used thermoluminescent phosphors to give the following results: LiF(TLD-100), 0.039%; $Li_2B_4O_7$:Mn, 0.073% (both corrected for supralinearity); CaF_2:Mn, 0.44%; and $CaSO_4$:Mn, 1.2%. The method of measurement involved calibrating a detector, which consisted of a narrow bandpass filter in conjunction with a photomultiplier, by means of the light of a standard lamp diffusely reflected from a MgO button having the same size, shape, and position as the phosphor-bearing planchet. A correction was made to account for the fact that the phosphor samples were not Lambertian sources.

DD FORM 1 NOV 65 1473 (PAGE 1)

S/N 0101-807-6801

Security Classification

14. KEY WORDS	LINK A ROLE	LINK A WT	LINK B ROLE	LINK B WT	LINK C ROLE	LINK C WT
Dosimetry						
Thermal luminescence						
Solid state						
Lithium fluoride (TLD-100)						
Lithium borate-manganese						
Calcium fluoride-manganese						
Calcium sulfate-manganese						
Lambertian source						